Computer Assisted Mechanics and Engineering Sciences, 14: 497–507, 2007.

Neural analysis of elastoplastic plane stress problem with unilateral constraints

Ewa Pabisek
Institute for Computational Civil Engineering, Cracow University of Technology
ul. Warszawska 24, 31-155 Kraków, Poland

(Received May 9, 2006)

The paper is a development and continuation of paper [8] where the Panagiotopoulos approach was extended for the elastoplastic analysis. In case of elastic analysis the parameters of the Hopfield–Tank Neural Network (HTNN) are calibrated only once but the updating of the elastoplastic stiffness matrix needs an iteration of HTNN and FE system. The main problem is the matrix condensation repeated for each iteration step of the Newton–Raphson method. Besides all the improvements proposed in [15], a new interacting program has been implemented which enables a significant decrease of the processing time (number of iterations) in comparison with the time achieved in [8]. The results of the extensive numerical analysis are discussed for a tension perforated strip with a rigid bolt placed frictionlessly in a circular hole in the middle of the strip.

Keywords: neural network, finite element method, elastoplastic problem, unilateral constraints

1. Introduction

Artificial neural networks (ANNs) have been successfully applied in the analysis of numerous problems of mechanics of structures and materials [13, 16]. In [17] the attention was turned on two fields of ANNs applications. The first one is related to the use of ANN as a new independent computational tool. The other field is associated with the complementary features of ANNs to the finite element method (FEM) and formulation of the hybrid FEM/ANN systems in which ANNs are used as numerically efficient subsystems or procedures. This approach corresponds to new trends in the computational structures technology where various hybrid systems with neural parts are pointed out as very promising prospects [7].

In hybrid FEM/ANN programs feed-forward, multilayer and error back-propagation neural networks (called BPNN in [13, 16, 17]) are applied. BPNNs are usually used at the Gauss points for the implicit modelling of material equations. cf. e.g. [3, 4, 8].

In the papers [5, 10] a recurrent network was applied in the interface zone. In this concept the Hopfield–Tank network (HTNN) was applied for modelling unilateral constraints using the Panagiotopoulos approach [13]. In this approach, called PA for short, HTNN evolutionary equations are transformed to a set of ordinary differential equations which formulate the FEM as an initial value problem. This idea can be expressed as the application of HTNN analog in FEM.

PA was successfully applied to the analysis of problems with unilateral constraints related to fracture mechanics [5, 10], analysis of elastoplastic frames [1], delamination of composites [6] and identification of yield surfaces [11].

In case of linear elastic problems the parameters of HTNN analog are computed only once, i.e. at the beginning of computations when FEM quantities are formulated. Even in the analysis of simple cases the increase of numerical efficiency of PA needs a number of modifications which were discussed in [15].

In the present paper three problems are considered. The first one is related to the application of PA to the analysis of elastoplastic problems with unilateral constraints. Using an incremental FE formulation the HTNN analog parameters have to be updated for each iteration step of the Newton–Raphson method. That means, in fact, an interaction of the FE program and the HTNN analog. The second problem corresponds to the analysis of a frictionless problem with an unknown contact zone. Following papers [5, 10] an original set of FE incremental equations is condensed to DOFs corresponding to unilateral constraints. This approach, discussed in [15], becomes much more complicated in case of elasto-plastic problems. It was stated in [8] that the condensation of DOFs at each Newton–Raphson iteration is very time consuming so a number of improvements is needed. They induce the third group of problems related to modification of numerical tools discussed in [8].

A novelty of the presented paper is a much more efficient FE program, written especially from the viewpoint of the condensation procedure. An automatic renumbering of DOFs leads to a narrow semi-band of the considered stiffness method. Another improvement corresponds to a simple adaptive scheme for the load factor step.

A higher numerical efficiency of the FEM/HTNN hybrid program than the one achieved in [15] is shown on an example of a tension perforated strip with a rigid bolt placed frictionlessly in the hole. A number of conclusions, valuable for the future research, can be drawn on the basis of extended numerical analysis.

2. HTNN AND FEM FORMULATIONS

2.1. The Panagiotopoulos approach

The Hopfield–Tank Neural Network (HTNN) was formulated for continuous variables. HTNN appears to be especially useful for the analysis of mathematical programming problems [13].

In Fig. 1 the HT network feedbacks are shown. HTNN is ready for operation after the network parameters w_{ij} and I_i are specified, i.e. computed in the so-called storage phase. The network operates in the retrieval phase in a dynamic way. This means that after introduction of initial values of inputs $x_i(0)$, their subsequent values $x_i(s)$ are computed recurrently. The iteration is continued until the stable state of the network equilibrium is reached. HTNN can be considered as

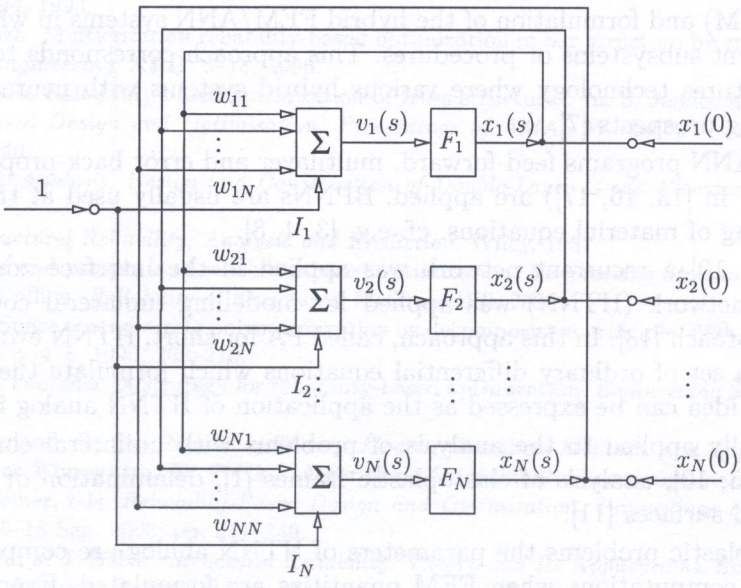

Fig. 1. Architecture of HTNN

a dynamic system and Lyapunov's theory can be usefully applied. For HTNN the following energy function is defined [13],

$$E(\mathbf{x}(s)) = -\frac{1}{2}\sum_{i=1}^{N}\sum_{j=1}^{N} w_{ij}x_i(s)x_j(s) - \sum_i I_i x_i(s) + \sum_i \frac{1}{R_i}\int_0^{x_i} F_i^{-1}(x)\,\mathrm{d}x\,, \tag{1}$$

where: s – iteration step, F_i – activation functions, $R_i > 0$ – network parameters. Function (1) is also valid for the dynamic, continuous in time, process which is described by a set of ordinary equations,

$$C_i\frac{\mathrm{d}v_i}{\mathrm{d}t} = -\frac{\partial E}{\partial x_i}\Big|_{x_i(t)} = -\frac{v_i}{R_i} + \sum_{j=1}^{N} w_{ij}x_j + I_i\,, \tag{2}$$
$$x_i(t) = F_i(v_i(t)) \qquad \text{for} \quad i = 1,\ldots,N\,,$$

where: $C_i > 0$ – network parameters. HTNN is an analog of the electrical network where: w_{ij} are conductances, I_i – current sources, x_i – potentials, C_i – capacities and R_i – resistances, cf. [13]

Equations (2) are called HTNN evolutionary equations. The stable equilibrium state is defined by the following criteria,

$$\min E(t) = 0 \quad \Longleftrightarrow \quad \frac{\mathrm{d}\mathbf{x}}{\mathrm{d}t} = \mathbf{0}\,. \tag{3}$$

In papers [5, 10] by Panagiotopoulos and his associates it was proved that HTNN can be specified for the analysis of quadratic programming problems with

a) bilateral constraints

$$\min\left\{\frac{1}{2}\mathbf{Q}^T\mathbf{K}\mathbf{Q} - \mathbf{P}^T\mathbf{Q}\right\}\,, \tag{4a}$$

b) unilateral constraints

$$\min\left\{\frac{1}{2}\mathbf{Q}^T\mathbf{K}\mathbf{Q} - \mathbf{P}^T\mathbf{Q}\Big|\mathbf{Q} \geq \mathbf{0}\right\}\,, \tag{4b}$$

where the FE notation is used: $\mathbf{K} \in \mathcal{R}^N \times \mathcal{R}^N$ – stiffness matrix, $\mathbf{P}, \mathbf{Q} \in \mathcal{R}^N$ – nodal forces and displacement vectors, respectively.

HTNN parameters are related to the components of FE matrices,

$$w_{ij} = w_{ji} = \begin{cases} -K_{ij} & \text{for} \quad i \neq j\,, \\ -K_{ij} + 1/R_i & \text{for} \quad i = j\,, \end{cases} \qquad I_i = P_i\,. \tag{5}$$

Variables x_i are specified in (1) and (2) using activation functions corresponding to types of constraints,

a) identity activation function for bilateral constraints,

$$x_i = Q_i = F_i(v_i) = v_i\,, \tag{6a}$$

b) piecewise-linear activation function for unilateral constraints,

$$x_i = Q_i = F_i(v_i) = \begin{cases} v_i & \text{for} \quad v_i \geq 0\,, \\ 0 & \text{for} \quad v_i < 0\,. \end{cases} \tag{6b}$$

After adopting $C_i = 1$ for $i = 1,\ldots,N$ and substituting Eqs. (5) and (6), Eqs. (2) take the form

$$\frac{\mathrm{d}\mathbf{v}}{\mathrm{d}t} = -\mathbf{K}\mathbf{Q} + \mathbf{P} \equiv \mathbf{R}_t\,, \tag{7}$$

where: $\mathbf{R}_t$ – vector of residuals at time t. In what follows, Eq. (7) is called HTNN analog.

2.2. HTNN and FEM in plasticity

The asymptotically stable equilibrium state of HTNN corresponds to the equilibrium state of FEM system

$$\frac{d\mathbf{v}}{dt} = \mathbf{R} \longrightarrow \mathbf{0} \quad \Longrightarrow \quad \mathbf{KQ} = \mathbf{P}\,, \tag{8}$$

where: $\mathbf{R} = \mathbf{P} - \mathbf{KQ}$ – vector of residual nodal forces. This means that instead of the analysis of algebraic problem (8), the initial value problem (7) is considered, corresponding to the simple gradient method of solution of the set of algebraic equations. In case of linear FEM formulation, stiffness matrix $\mathbf{K}$ and reference load vector $\mathbf{P}^*$ are fixed. The HTNN analog, i.e. analysis of the initial value problem (7), can be used for different values of load factor Λ in the vector of nodal loads $\mathbf{P} = \Lambda\,\mathbf{P}^*$. This approach can be used efficiently for the analysis of linear elasticity problems with unilateral constraints, cf. [15].

The analysis of elastoplastic problems by the HTNN analog is much more difficult since the network parameters, corresponding to FEM matrices $\mathbf{K}$ and $\mathbf{P}$ in (7), are influenced by the yielding process. Instead of Eq. (8) the incremental FE equation is used, cf. [12],

$$\mathbf{K}_T \Delta\mathbf{Q} = \Delta\Lambda \cdot \mathbf{P}^* + \mathbf{R}\,, \tag{9}$$

where: $\mathbf{K}_T$ – tangent stiffness matrix, $\Delta\mathbf{Q}$ – increment of nodal displacements vector, $\Delta\Lambda$ – increment of load factor, $\mathbf{P}^*$ – reference nodal loads vector.

Equation (9) is solved iteratively using various control parameters [2]. Let us assume load control and the load factor increments $\Delta_m\Lambda$ and iteration steps it for solving a sequence of linearized FE equations

$${}_m\mathbf{K}^{(it-1)} \Delta\Delta\mathbf{Q}^{(it)} = \alpha^{(it)} \Delta_m\Lambda \cdot \mathbf{P}^* + (1 - \alpha^{(it)})\, {}_m\mathbf{R}^{(it-1)}\,, \tag{10}$$

where: ${}_m\mathbf{K}^{(it-1)} = \mathbf{K}_T({}_m\mathbf{Q}^{(it-1)})$, ${}_m\mathbf{R}^{(it-1)} = \mathbf{R}({}_m\mathbf{Q}^{(it-1)})$ – tangent stiffness matrix and vector of residual forces, updated for the vector of total displacements

$${}_m\mathbf{Q}^{(it-1)} = {}_{m-1}\mathbf{Q} + \sum_{k=1}^{it-1} \Delta\Delta\mathbf{Q}^{(k)}\,, \tag{11}$$

and the parameter $\alpha^{(it)}$ to be

$$\alpha^{(it)} = \begin{cases} 1 & \text{for predictor at} \quad it = 1\,, \\ 0 & \text{for corrector at} \quad it > 1\,. \end{cases} \tag{12}$$

It was stated in papers [5, 10, 15] that the iteration process converges more quickly in case of unilateral constraints. That is why elimination of bilateral constraints and corresponding condensation of the stiffness matrix is recommended. Let us assume that the condensed system has $n \ll N$ degrees of freedom and the corresponding stiffness matrix and vectors in $\mathcal{R}^n$ space are written in small letters, i.e. $\mathbf{k}, \mathbf{q}, \mathbf{p}, \mathbf{r}$.

2.3. Condensation of bilateral DOFs

The displacement vector $\mathbf{Q} \in \mathcal{R}^N$ is split into subvectors $\mathbf{q} \in \mathcal{R}^n$ and $\mathbf{Q}_C \in \mathcal{R}^{N-n}$,

$$\mathbf{Q} = \{\mathbf{q},\ \mathbf{Q}_C\}\,, \tag{13}$$

where $\mathbf{q}$ – vector corresponding to predicted unilateral constraints. For the sake of simplicity, Eq. (9) is written in the form corresponding to Eq. (13),

$$\begin{bmatrix} \mathbf{K}_A & \mathbf{K}_B \\ \mathbf{K}_B^T & \mathbf{K}_C \end{bmatrix} \begin{bmatrix} \Delta\mathbf{q} \\ \Delta\mathbf{Q}_C \end{bmatrix} = \begin{bmatrix} \Delta\mathbf{P}_A \\ \Delta\mathbf{P}_C \end{bmatrix}. \tag{14}$$

After evident manipulations the following relations are obtained for the condensed system of n degrees of freedom,

$$\mathbf{k}\,\Delta\mathbf{q} = \Delta\mathbf{p}, \qquad \text{where:} \quad \mathbf{k} = \mathbf{K}_A - \mathbf{K}_B\,\mathbf{K}_C^{-1}\,\mathbf{K}_B^T, \quad \Delta\mathbf{p} = \Delta\mathbf{P}_A - \mathbf{K}_B\,\mathbf{K}_C^{-1}\,\Delta\mathbf{P}_C, \tag{15}$$

and for returning to original system

$$\Delta\mathbf{Q}_C = -\mathbf{K}_C^{-1}\,\mathbf{K}_B^T\,\Delta\mathbf{q} + \mathbf{K}_C^{-1}\,\Delta\mathbf{P}_C. \tag{16}$$

In paper [15], the simple gradient method, used in [5, 10], was replaced by the conjugate gradient method so the evolutionary equation of the condensed system takes the form

$$\frac{\mathrm{d}\mathbf{v}}{\mathrm{d}t} = \mathbf{r}_t - \beta_t \cdot \mathbf{r}_{t-1} \qquad \text{for} \quad \beta_t = \frac{\mathbf{r}_t^T \cdot \mathbf{r}_t}{\mathbf{r}_{t-1}^T \cdot \mathbf{r}_{t-1}}, \tag{17}$$

where $\mathbf{r}_t$ is the vector of residual forces at the time instant t,

$$\mathbf{r}_t = -\mathbf{k}({}_m\mathbf{q}^{(it-1)})\Delta\Delta\mathbf{q}_t + \alpha^{(it)}\Delta_m\Lambda \cdot \mathbf{p}^*(1-\alpha^{(it)})\left({}_m\Lambda\mathbf{p}^* - \mathbf{f}({}_m\mathbf{q}^{(it-1)})\right). \tag{18}$$

The stiffness matrix ${}_m\mathbf{k}^{(it-1)}$ and the vector of internal forces ${}_m\mathbf{f}^{(it-1)}$ are to be updated for each iteration step it on the system level. These values are fixed for the HTNN analysis at each it step.

In case of the modified Newton–Raphson method the stiffness matrix is updated only several times at the beginning of each load level m, i.e. ${}_m\mathbf{k} = \mathbf{k}({}_m\mathbf{q}^{(s)})$, where s denotes the number of it after which the stiffness matrix is fixed.

The main problem of condensation is the inversion of matrix $\mathbf{K}_C$ shown in (14). A numerically efficient procedure of the system decomposition has been worked out on the basis of renumbering of DOFs, which leads to the minimal width of the semi-band of matrix $\mathbf{k}$.

3. Analysis of a perforated tension strip with a frictionless contact zone

3.1. Assumptions and data

The computational method FEM-HTNN, depending on the interaction of FEM and HTNN, is illustrated on an example of a perforated tension strip which is considered in many papers as a bench-mark type problem, cf. [14]. Two special cases are discussed: A) a strip with a free boundary of the hole, B) a rigid bolt is fitted to the hole and frictionless contact zone occurs under the applied load, uniformly distributed along the external boundaries, Fig. 2a.

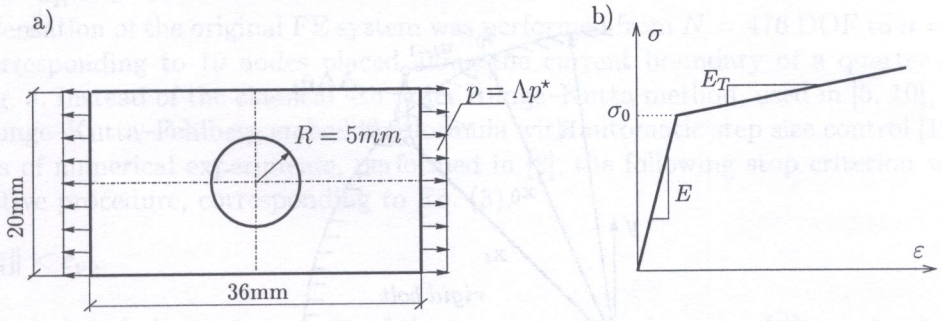

$E = 7 * 10^4$ N/mm^2, $E_T = 2.24 * 10^3$N/mm^2, $\chi = E_T/E = 0.032$,
$\sigma_0 = 243$N/mm^2, $\nu = 0.2$, $p^* = 121.5$N/mm^2

Fig. 2. Geometrical, load and material data for a perforated strip

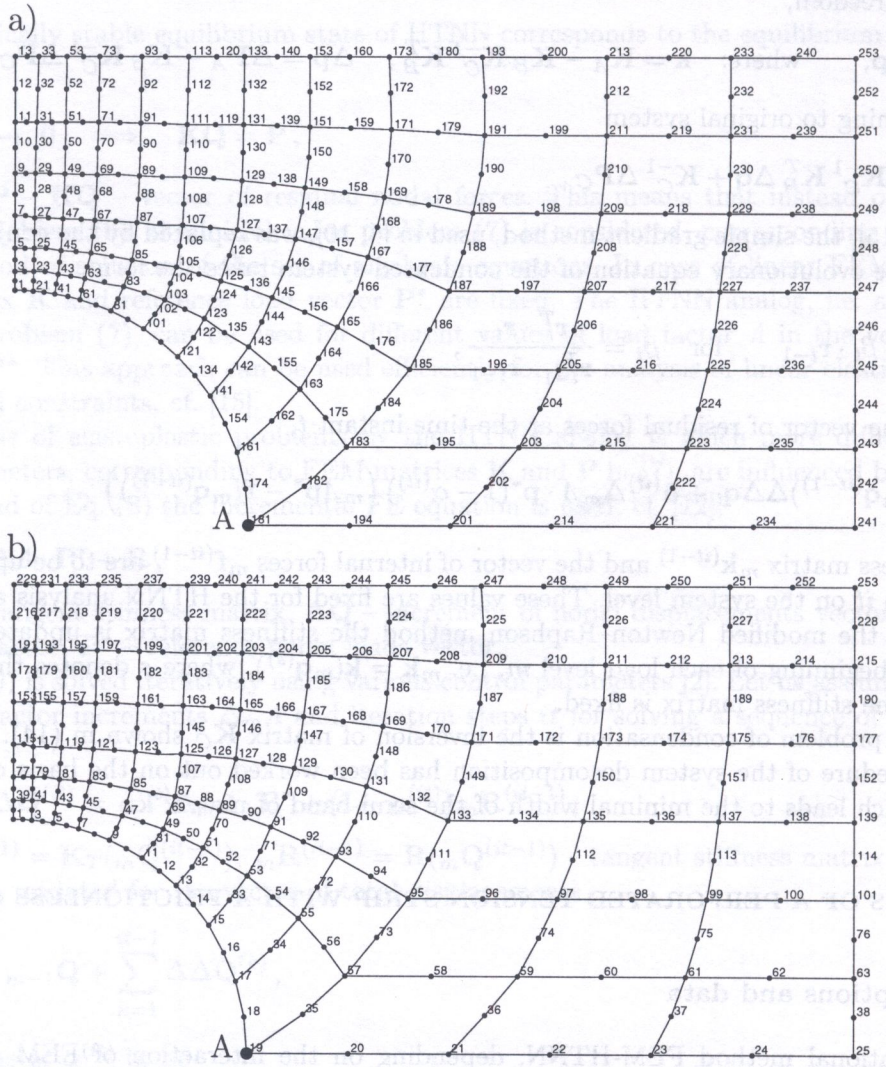

Fig. 3. FE mesh for a quarter of the strip: a) Numeration of nodes for the hole free boundary and application of FEM only, b) Numbering of nodes for FEM-HTNN interaction

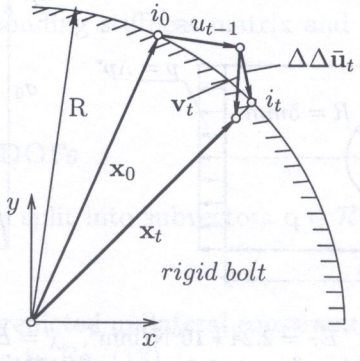

Fig. 4. Increment of the vector of unilateral displacements of node i at a rigid bolt

The strip is made of a homogeneous, isotropic material with the Huber–Misses–Hencky yield surface and the linear, isotropic strain hardening, corresponding to data of uniaxial tension shown in Fig. 2b. Because of double symmetry only a quarter of the strip is analysed. The 8-node isoparametric plane FEs with four Gauss points of reduced integration are used. The FE system shown in Fig. 3 has $N = 2 \cdot 253 - (7 + 13) = 476$ DOF, where $(7 + 13) = 20$ DOF correspond to the supports at the symmetry axes. In case B), i.e. for the strip with a rigid bolt, the frictionless contact is assumed. Because of the curved contact boundary the constraint condition is formulated in the form corresponding to node i of the displacement vector $\mathbf{u}$, cf. Fig. 4,

$$\Delta\Delta\mathbf{u}_t = \begin{cases} \mathbf{v}_t & \text{for } |\mathbf{x}_t| \geq R, \\ \Delta\Delta\bar{\mathbf{u}}_t & \text{for } |\mathbf{x}_t| < R, \end{cases} \tag{19}$$

where

$$\mathbf{x}_t = \mathbf{x}_0 + \mathbf{u}_{t-1} + \mathbf{v}_t\,, \qquad \Delta\Delta\bar{\mathbf{u}}_t = \frac{R}{|\bar{\mathbf{x}}_t|} - \mathbf{x}_0 - \mathbf{u}_{t-1}\,. \tag{20}$$

To make it easier the node index i and iteration superscript it, cf. Eq. (18), are omitted in Eqs. (19), (20) and in Fig. 4.

3.2. Numerical analysis

The computations were carried out under the load control $\tau = \Lambda$ for the load factor value up to $\Lambda = 2.0$. Two changes of load step size were used: 1) constant increment of load factor $\Delta\Lambda$, 2) adaptive increments $\Delta_m\Lambda$.

A very simple adaptation formula is assumed for $\Delta_m\Lambda$,

$$\Delta_m\Lambda = \begin{cases} \Delta_{m-1}\Lambda/2 & \text{for } Itm > It+\,, \\ \Delta_{m-1}\Lambda & \text{for } It- \leq Itm \leq It+\,, \\ \Delta_{m-1}\Lambda * 2 & \text{for } Itm < It-\,, \end{cases} \tag{21}$$

where: Itm – number of iteration for the m-th step of the Newton–Raphson method; $It-, It+$ – prescribed number of iterations. Itm corresponds to the satisfaction of the following convergence conditions, cf. [12],

$$\|\Delta\Delta\bar{\mathbf{Q}}\| < \varepsilon_Q \qquad \text{and} \qquad \|\bar{\mathbf{R}}\| < \varepsilon_R\,, \tag{22}$$

where: $\|(\bar{\cdot})\|$ – norms of dimensionless vectors.

In case of the considered quarter of the strip it was assumed in (21) and (22) that $It- = 4$, $It+ = 7$, $\varepsilon_Q = \varepsilon_R = 1 \cdot 10^{-4}$.

The condensation of the original FE system was performed from $N = 476$ DOF to $n = 2*19-1 = 37$ DOF, corresponding to 19 nodes placed along the current boundary of a quarter of the strip shown in Fig. 3. Instead of the classical 4th order Runge–Kutta method, used in [5, 10], the 5th and 6th order Runge–Kutta–Fehlberg embedding formula with automatic step size control [15] was used. On the basis of numerical experiments, performed in [8], the following stop criterion was assumed for the iterative procedure, corresponding to Eq. (3),

$$\max_i \|\Delta v_i\| < \varepsilon_v\,, \tag{23}$$

where: $\Delta v_i = (v_i)_t - (v_i)_{t-1}$ – increment of the component $i = 1, \cdots, n$ of the vector v in Eq. (17). In the computations associated with the problem considered the admissible error $\varepsilon_v = 1 \cdot 10^{-10}$ was used. The computations were run on a PC class computer, with Linux system. In Table 1 the results of computations are listed for two cases A) and B), i.e. for a strip with no bolt and with one the bolt, respectively. The case A) was analysed by means of pure FEM program, then by the hybrid

Table 1. Total number of iterations NR in the Newton–Raphson method, total number of iterations HT by HTNN and number of load factor steps M for initial increment $\Delta_1 \Lambda$ (D – divergence of the iteration process).

Steps of load factor		Case A) hole with no bolt (free boundary of hole)				Case B) hole with a bolt (frictionless contact boubd.)	
		FEM	FEM/BPNN	FEM -HTNN	FEM/BPNN -HTNN	FEM -HTNN	FEM/BPNN -HTNN
$\Delta\Lambda = 0.1$	NR	87	67	87	75	88	82
	HT	–	–	161818	196231	140709	183797
$\Delta\Lambda = 0.2$	NR	48	40	47	D	47	D
	HT	–	–	94441		82484	
$\Delta\Lambda = 0.1$	NR	145	112	140	D	140	D
mNR	HT	–	–	248635		207201	
$\Delta\Lambda = 0.2$	NR	84	D	86	D	85	D
mNR	HT	–		168140		135836	
$\Delta_1\Lambda = 0.1$	NR	46	72	47	39	30	58
	HT	–	–	103417	114315	55104	150305
	M	10	16	13	9	7	14
$\Delta_1\Lambda = 0.2$	NR	40	38	40	41	40	59
	HT	–	–	99897	100823	77980	144710
	M	8	8	8	8	8	8
$\Delta_1\Lambda = 0.4$	NR	41	58	35	56	43	58
	HT	–	–	85823	184435	80954	148979
	M	8	13	6	13	8	13
$\Delta_1\Lambda = 1.0$	NR	31	44	21	43	24	44
	HT	–	–	75738	149051	52531	125173
	M	5	9	5	9	4	9

program with the neural procedure taken from [14]. The same case was analysed by the hybrid program FEM-HTNN and FEM/BPNN-HTNN.

The case B), i.e. the strip with a rigid bolt, was analysed by the programs FEM-HTNN and FEM/BPNN-HTNN.

In both cases the fixed load steps $\Delta\Lambda = 0.1, 0.2$ were applied and after $M = 20, 10$ steps, respectively, the load factor reached the value $\Lambda = 2.0$. The initial steps $\Delta_1\Lambda = 0.1, 0.2, 0.4, 1.0$ were used in case of application of the adaptive formula (21). The numbers NR and HT correspond to the total number of iterations in the Newton–Raphson method and in the HTNN analog, respectively. In case of the adaptive load step the number of load factor increments M is shown.

For the fixed values of $\Delta\Lambda = 0.1, 0.2$ the results of computations for the modified Newton–Raphson method are shown as ${}_m$NR. After a number of experiments performed for $\Delta\Lambda = 0.1$ it was stated that the lowest number of iterations NR could be obtained for fixing the stiffness matrix ${}_m\mathbf{k}^{(s)}$ after the first $s = 3$ iterations for each load increment m. In case of the divergent iteration process the capital D is shown in Table 1.

3.3. Discussion of results

The computations performed at different load factor increments $\Delta\Lambda$ did not affect significantly the results corresponding to the final load value $\Lambda = 2.0$. It was stated that for the equilibrium paths shown in Fig. 5 values of displacements $u_A(\Lambda = 2.0)$ had the same three significant digits independent of values of $\Delta\Lambda$ or $\Delta\Lambda_1$.

In Fig. 5 equilibrium paths $\Lambda(u_A)$ are shown for the strips with and without a rigid bolt. It is evident that the strip with a rigid bolt is stiffer than the strip with no bolt. After unloading the

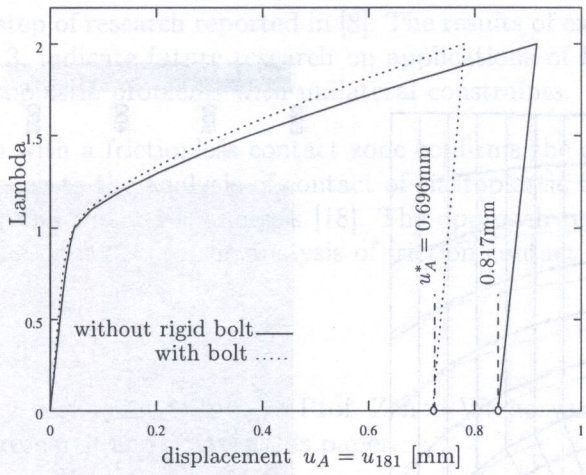

Fig. 5. Equilibrium paths $\Lambda(u_A)$ for a perforated strip with and with no rigid bolt placed in the strip hole

permanent displacement of the strip with bolt $u_{\mathrm{A}}^* = 0.72$mm is about 15% smaller than displacement $u_A^* = 0.84$ mm of the strip with a bolt.

In Figs 6a,b the deformed strips are shown. As can be seen, the contact takes place only along four FEs. In Figs 6c,d yielding zones are shown. They are affected, of course, by the contact boundary of the strip and bolt.

The application of an improved condensation procedure enables a significant decrease of the number of iterations HT of the case B) analysis. It was stated in [13] $\Delta\Lambda = 0.1$ the total number of iteration was about HT = 24–30 for the adaptive load factor (cases $\Delta\Lambda = 0.1, 1.0$)

The next conclusions correspond to the results in [5, 10, 15]. The analysis of constraints by the FEM and HTNN interaction i causes a significant increase of iterations NR, e.g. compare the results obtained for case A) by programs FEM and FEM/BPNN vs. results by means of FEM/BPNN-HTNN. The activation of unilateral constraints, i.e. appearance of contacts between the strip and bolt, causes the decrease of iteration numbers HT. The advantages resulting from the incorporation of the BPNN procedure into the FEM program (hybrid program FEM/BPNN) are not so evident as it was concluded in [14]. In many cases listed in Table 1 the results obtained by means of the hybrid programs FEM/BPNN and FEM/BPNN-HTNN are worse than those by the programs FEM and FEM-HTNN. A probable reason is that the BPNN used in [14] has wider generalization features than those needed for the analysis at longer and adaptive load factor step size.

There are no advantages of the application of the modified Newton–Raphson method ($_m$NR). The simplest version of $_m$NR, corresponding to single updating of the structural stiffness matrix per one load step, leads to early divergence of the iteration process. The updating at the first three iterations per one $\Delta\Lambda$ can also be insufficient to improve the results obtained by $_m$NR vs. results by the classical NR method.

4. Conclusions

1. The Panagiotopoulos approach is developed from the viewpoint of the elastoplastic analysis. The approach can be interpreted as an interaction of two programs, i.e. a FEM program and HTNN numerical analog, to solve the incremental set of FE equations with unilateral constraints.

2. The procedure of FE stiffness matrix condensation is the most time consuming procedure so the optimization of this procedure can give significant reduction of iteration number.

3. The application of a hybrid program FEM/BPNN needs deeper recognition from the viewpoint of sufficient generalization features of the neural procedure used in [14] for the simulation of the Return Mapping Algorithm.

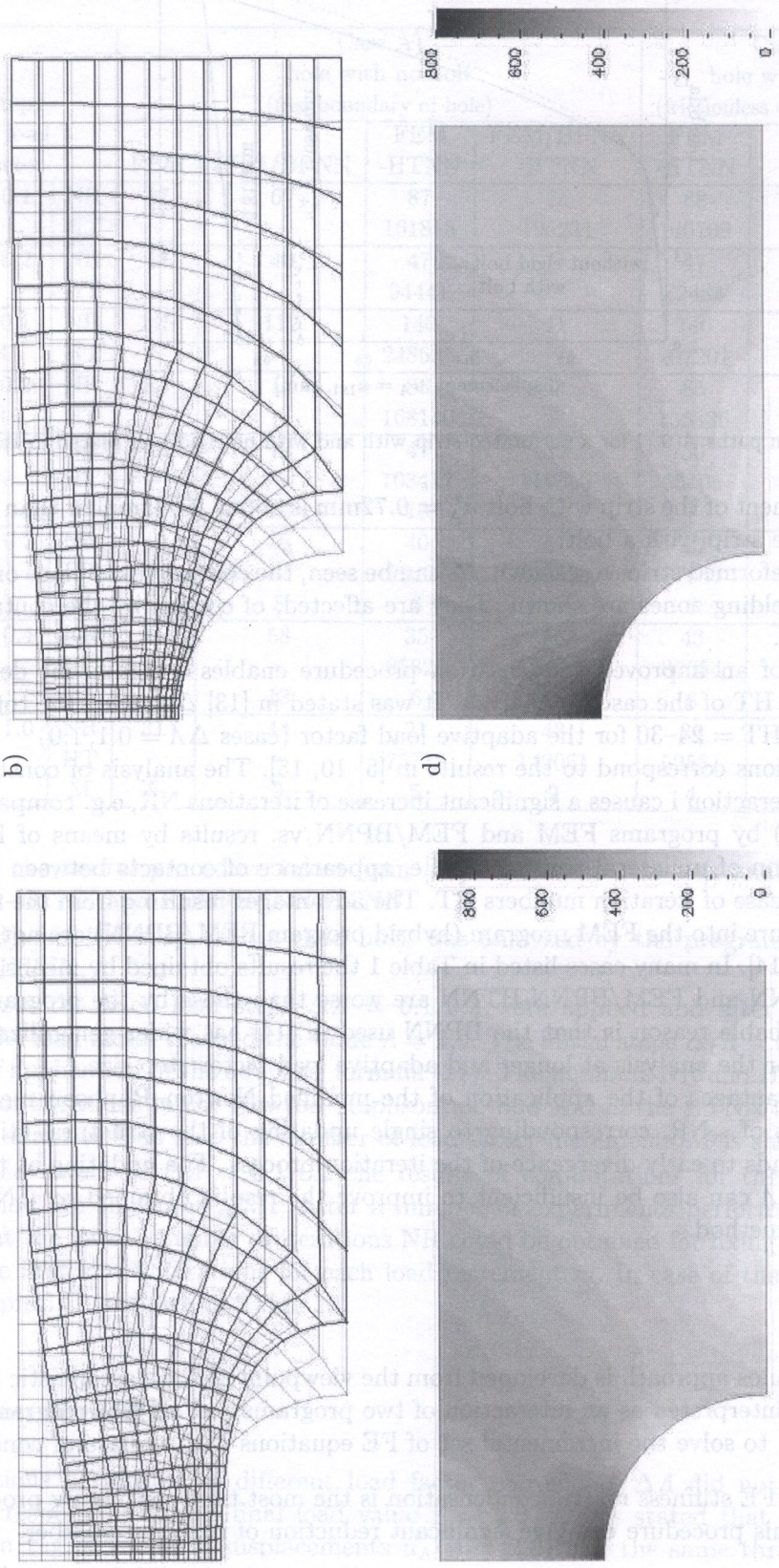

Fig. 6. Deformations of strips at load factor $\Lambda = 2.0$: a) Strip with no bolt, b) Strip with a rigid bolt; Distribution of effective stresses σ_e: c) Strip with no bolt, d) Strip with a rigid bolt

4. The paper is the next step of research reported in [8]. The results of extended numerical analysis, discussed in Section 3.3, indicate future research on applications of Panagiotopoulos' approach to the analysis of elastoplastic problems with unilateral constraints.

5. The analysis of a strip with a frictionless contact zone confirms the advantages of the modified Panagiotopoulos approach to the analysis of contact of elastoplastic bodies. These problems are one of more complex problems of FE analysis [18]. The approach related to the application of HTNN analog opens the door also to the analysis of friction contact problems [9].

ACKNOWLEDGMENTS

I would like to express my very great thanks to Prof. Zenon Waszczyszyn for his suggestions and help in the realisation of research and writing this paper.

REFERENCES

[1] A.V. Avdelas *et al.* Neural networks for computing in the elastoplastic analysis of structures. *Mechanica*, **30**: 1–15, 1995.

[2] G. Engeln-Müllges, F. Uhlig. *Numerical Algorithms with C.* Springer, Berlin–Heidelberg, 1996.

[3] J. Ghaboussi *et al.* Knowledge-based modeling of material behavior with neural networks. *ASCE J. Engrg. Mech.*, **117**: 132–153, 1991.

[4] Ł. Kaczmarczyk, Z. Waszczyszyn. Neural procedures for the hybrid FEM/NN analysis of elastoplastic plates. *Comput. Assisted Mech. Engrg. Sci.*, **12**: 379–391, 2005.

[5] S. Kortesis, P.G. Panagiotopoulos. Neural networks for computing in structural analysis — methods and prospects of applications. *Int. J. Num. Meth. Engrg.*, **36**: 2305–2318, 1993.

[6] E.S. Mistakidis, P.G. Panagiotopoulos. Numerical treatment of problems involving nonmonotone boundary or strain–stress laws. *Comput. Struct.*, **64**: 533–565, 1997.

[7] A.K. Noor. Computational structures technology: leap frogging into the twenty-first century. *Comput. Struct.*, **73**: 1–31, 1999.

[8] E. Pabisek, Z. Waszczyszyn. Neural networks in the analysis of elastoplastic stress problem with unilateral constraints. In: B.H.V. Topping, ed., *Computational Engineering Using Metaphors from Nature*, pp. 1–6, Civil-Comp Press, Edinburgh, 2000.

[9] E. Pabisek, Z. Waszczyszyn. Hybrid FEM/NN analysis of friction contact of elastic and elastoplastic bodies. In *Proc. of Conf. on Numerical Methods in Continuum Mechanics*, pp. 1–12, Žilina, Slovak Republic, 2003. D&D Digital Printing Office.

[10] P.S. Theocaris, P.G. Panagiotopoulos. Neural networks for computing in fracture mechanics — methods and prospects of applications. *Comput. Methods Appl. Mech. Engrg.*, **106**: 213–228, 1993.

[11] P.S. Theocaris, P.G. Panagiotopoulos. Generalized hardening plasticity approximated via anisotropic elasticity: a neural network approach. *Comput. Methods Appl. Mech. Engrg.*, **125**: 123–139, 1995.

[12] Z. Waszczyszyn, Cz. Cichoń, M. Radwańska. *Stability of Structures by Finite Element Method.* Elsevier, Amsterdam–Tokyo, 1994.

[13] Z. Waszczyszyn, ed. *Neural Networks in the Analysis and Design of Structures.* CISM Courses and Lectures No. 404. Springer, 1999.

[14] Z. Waszczyszyn, E. Pabisek. Hybrid NN/FEM analysis of the elastoplastic plane stress problem. *Comput. Assisted Mech. Engrg. Sci.*, **6**: 177–188, 1999.

[15] Z. Waszczyszyn, E. Pabisek. Application of a Hopfield type neural network to the analysis of elastic problems with unilateral constraints. *Comput. Assisted Mech. Engrg. Sci.*, **7**: 757–765, 2000.

[16] Z. Waszczyszyn, L. Ziemiański. *Neural Networks in the identification analysis of structural mechanics problems.* CISM Courses and Lectures No. 469. Springer, 2005.

[17] Z. Waszczyszyn, L. Ziemiański. Neurocomputing in the analysis of selected inverse problems of mechanics of structures and materials. *Comput. Assisted Mech. Engrg. Sci.*, **13**: 125–159, 2006.

[18] P. Wriggers. *Computational Contact Mechanics.* John Willey & Sons, Chichester, UK, 2002.